

FIG 2. **A**, The median T_{react} in relation to the challenge dose. **B**, The median S_{wheal} in relation to the challenge dose. Both graphs (box plots) display the distribution of the data as follows: the median, the 25th and 75th percentiles (the boundary of the box), and the highest and lowest values (the whiskers above and below the box). All recipients were sensitized with donor serum 2, 3, and 4 (Table E1). The difference in the median T_{react} between all doses compared pairwise was statistically significant ($P \leq .003$) except for the difference between 1 g and 3 g of peanut ($P = .4$). The difference in the median S_{wheal} between the doses compared pairwise was statistically significant ($P \leq .001$) except for the differences between 1 g and 3 g of peanut ($P = .05$) and 10 g and 100 g of peanut ($P = .1$). The asterisks indicate that a reaction was negative.

(and as yet unknown) allergen(s) in the blood and then compare the plasma concentrations to *in vitro* histamine release from basophils or mast cells. Although all recipients demonstrated a positive skin prick test result to a crude peanut extract at the sites of the serum injections, an *in vitro* dose titration using basophils or mast cells would make little sense due to the lack of data on the nature and the concentration of the relevant allergen(s) in plasma. It should be noted that this study does not focus on the kinetics of the allergens and therefore does not address interesting questions such as the sensitivity of the setup, that is, how low concentrations of the allergen(s) that can be detected, but focus only on the dynamics of the reaction, that is, T_{react} and S_{wheal} .

If our data are transferrable to allergic patients, the results indicate that a 30-minute interval between doses in titrated oral peanut challenges in patients could be too short, particularly when the sIgE level or challenge dose is low. This is consistent with the study in peanut-allergic patients by Blumchen et al,¹ who found

that 71% of their participants showed objective symptoms after more than 30 minutes, with a median T_{react} of 55 minutes using a modified oral peanut challenge protocol with a 2-hour interval between dose steps.

Limitations of this study include that the experiments were carried out in nonallergic individuals; we cannot rule out fundamental differences in the regulatory pathways of the IgE-mediated response between individuals with allergy and individuals who have been passively sensitized. Furthermore, the events taking place in the gastrointestinal tract of individuals with allergy before systemic distribution of the allergen are bypassed in this model.⁷

We are truly grateful to all study participants (donors and recipients) who took part in the study.

Anja P. Mose, MD^{a,b}
Charlotte G. Mortz, MD, PhD^{a,b}
Esben Eller, MSc, PhD^{a,b}
Ulrik Sprogøe, MD, PhD^c
Torben Barington, MD, DMSc^c
Carsten Bindslev-Jensen, MD, PhD, DMSc^{a,b}

From ^aOdense Research Center for Anaphylaxis (ORCA), ^bthe Department of Dermatology and Allergy Center, and ^cthe Department of Clinical Immunology, Odense University Hospital, Odense, Denmark. E-mail: carsten.bindslev-jensen@rsyd.dk.

Conflicts of interest: C. G. Mortz has served on a board for Novartis and has received payment for lectures from Novartis and Sandoz A/S. C. Bindslev-Jensen has received a grant from Odense University Hospital Research Foundation, has consultant arrangements with Hal Allergy and Anergis, and has received payment for lectures from Hal Allergy and Thermofisher. The rest of the authors declare that they have no relevant conflicts of interest.

REFERENCES

- Blumchen K, Beder A, Beschoner J, Ahrens F, Gruebl A, Hamelmann E, et al. Modified oral food challenge used with sensitization biomarkers provides more real-life clinical thresholds for peanut allergy. *J Allergy Clin Immunol* 2014;134:390-8.
- Prausnitz C, Küstner H. Studien über uberempfindlicht. *Centralb Bakterial I Abt Orig* 1921;86:160-9.
- The Danish Blood Safety Directives (Bekendtgørelse nr 366 af 23/04/2012). Available at: <https://www.retsinformation.dk/Forms/R0710.aspx?id=141589>. Accessed July 8, 2013.
- Brunner M, Walzer M. Absorption of undigested proteins in human beings: the absorption of unaltered fish proteins in adults. *Arch Intern Med* 1928;42:172-9.
- Aoki T, Funai T, Kojima M, Adachi J. Absorption of egg antigens by the gut observed by oral Prausnitz-Küstner (Walzer) reaction in atopic dermatitis. *Acta Derm Venereol Suppl (Stockh)* 1989;144:100-4.
- Yokooji T, Hamura K, Matsuo H. Intestinal absorption of lysozyme, an egg-white allergen, in rats: kinetics and effect of NSAIDs. *Biochem Biophys Res Commun* 2013;438:61-5.
- Reitsma M, Westerhout J, Wichers HJ, Wortelboer HM, Verhoecx KC. Protein transport across the small intestine in food allergy. *Mol Nutr Food Res* 2014;58:194-205.

Available online February 8, 2017.
<http://dx.doi.org/10.1016/j.jaci.2016.11.034>

JAK1 gain-of-function causes an autosomal dominant immune dysregulatory and hypereosinophilic syndrome



To the Editor:

We describe the discovery and successful treatment of the first humans with a germline mutation in Janus kinase 1 (*JAK1*). The

janus kinase/signal transducers and activators of transcription (JAK/STAT) pathway plays an integral role in extracellular cytokine and growth factor signaling, as well as in controlling hematopoiesis and immune function.¹ The *JAK1* gain-of-function (GoF) mutation in this family caused a systemic immune dysregulatory condition, which improved dramatically with the application of precision medicine to target the exaggerated JAK1 function.

A mother and her 2 children (aged 2 and 6 years) had a unique clinical phenotype: liver cysts noted on prenatal ultrasound, severe atopic dermatitis, profound eosinophilia with eosinophilic infiltration of the liver and gastrointestinal tract, massive hepatosplenomegaly, autoimmune thyroid disease, and failure to thrive (Fig 1; see Table E1 in this article's Online Repository at www.jacionline.org). The mother has been significantly affected since birth with severe, treatment-resistant atopic dermatitis, moderate short stature, environmental allergies, asthma, and eosinophilia (range, $2.87\text{--}3.29 \times 10^9/\text{L}$; normal, $<0.5 \times 10^9/\text{L}$). Her 2 sons presented with a more extensive phenotype, with height and weight growth parameters markedly below the third percentile for age (Fig 1, D). All known causes of eosinophilia were excluded, including infections, drug reactions, and malignancy (including clonal eosinophilia associated with chronic eosinophilic leukemia or genetic abnormalities of *PDGFRA*, *PDGFRB*, and *FGFR1*). Serum levels of cytokines known to promote eosinophilia, specifically IL-3, IL-5, and GM-CSF, were not different from those in healthy controls. The dermatitis and peripheral eosinophilia were unresponsive to systemic corticosteroid therapy (oral prednisone 2 mg/kg/d) (Fig 1, B), and serum IgE levels were normal, emphasizing the differences between this phenotype and typical atopic dermatitis.

Whole-exome sequencing of the affected boys and their parents, combined with targeted Sanger sequencing, revealed that the mother and 2 boys were heterozygous for a mutation in *JAK1* c.1901C>A, resulting in an alanine to aspartate substitution at position 634 (A634D) (see Fig E1 in this article's Online Repository at www.jacionline.org). It was not found in the mother's parents, confirming it as a *de novo* mutation (Fig 1, A). The c.1901C>A mutation has not been reported by the Exome Aggregation Consortium, and the mutation did not affect *JAK1* mRNA or protein expression (see Fig E2, A and B, in this article's Online Repository at www.jacionline.org).

The p.A634D mutation lies within the inhibitory pseudokinase domain of JAK1 (Fig E1, B and C). p.A634 is highly conserved across species, suggesting an important functional role (Fig E1, B). To characterize the *JAK1* p.A634D mutation, HEK293 cells were transfected with wild-type *JAK1*, *JAK1* c.1901C>A, or an empty vector. STAT1 and JAK1 activation was higher in cells containing the c.1901C>A vector at baseline and following stimulation (Fig 2, A and B). Pretreatment with ruxolitinib (an approved JAK1/2 inhibitor) decreased the phosphorylation of both STAT1 and JAK1 more effectively in cells expressing wild-type than mutant *JAK1*.

To confirm the GoF phenotype in primary patient cells, we quantified JAK1 activity in 2 cell types: immortalized B cells and primary CD3⁺ T cells. At baseline and following stimulation, patient B cells displayed increased levels of STAT1 phosphorylation ($P < .05$ and $P < .01$, respectively). Pretreatment with ruxolitinib significantly decreased this responsiveness (Fig 2, C, and Fig E2, C). Validating this result, we examined the patients' primary T cells using flow cytometry. Following stimulation with IL-6,

JAK1 c.1901C>A T cells demonstrated enhanced phosphorylation of STAT3 in a time- ($P < .05$) and dose-dependent ($P < .005$) manner (Fig 2, D and E).

Given the promising results showing that ruxolitinib dampens exaggerated JAK1 signaling caused by the c.1901C>A mutation (Fig 2), coupled with severe failure to thrive and intractable pruritus, the 2 affected children began treatment with ruxolitinib at 50 mg/m²/dose orally twice daily.² To avoid confounding, no other treatments were given. Within 2 weeks, they showed subjective improvement in their pruritus, appetite, and sleep patterns. After 1 month of therapy, they were gaining weight and had significantly reduced eosinophilia, together with clinical resolution of their dermatitis and hepatosplenomegaly (Fig 1, B and D).

To define the molecular response to ruxolitinib treatment, we repeated the functional flow cytometry assessment of JAK/STAT signaling. After treatment, the levels of pSTAT3 stimulated by IL-6 were significantly decreased compared with both the healthy controls ($P < .0005$) and pretreatment *JAK1* c.1901C>A cells ($P < .0001$) (Fig 2, E).

Germline GoF mutations in *JAK1* have never been previously reported in humans. There are at least 3 compelling lines of evidence supporting the assertion that *JAK1* p.A634D is a GoF mutation. First, *JAK1* p.A634D has been identified as a somatic mutation in malignant conditions and several groups have established the GoF phenotype.³⁻⁷ Second, using transfection experiments we confirm that the *JAK1* c.1901C>A plasmid triggers a higher level of downstream pSTAT1 activity than does wild-type *JAK1*, and this increased activity is less effectively inhibited with ruxolitinib (Fig 2, A). Third, using both patient B cells and primary T cells, we identified increased STAT1/3 activation following cytokine stimulation in the presence of the p.A634D mutation (Fig 2, C-E). Moreover, 2 recently developed mouse models with a *Jak1* GoF mutation share a number of similarities with the human phenotype, including skin inflammation, activation of the IL-6-JAK-STAT pathway, liver and spleen abnormalities, and autoimmune disease.^{3,8,9} Our observation that JAK1/2 inhibition with ruxolitinib resolved the severe dermatitis associated with the human *JAK1* GoF mutation, combined with the mechanistic insights from mouse models,⁸ provides further justification for targeting JAK1 in the treatment of atopic dermatitis.

Although the clinical response to ruxolitinib in the children has been transformative for the affected family, little is known about the consequences of long-term exposure to ruxolitinib, particularly in pediatric patients. Given the pivotal role of JAK-STAT signaling in hematopoiesis, a degree of reversible myelosuppression is expected, and we observed anemia that normalized after dose reduction. Ruxolitinib has also been associated with serious infections; all febrile illnesses in our patients have been carefully assessed, but no serious infections have occurred. Ultimately, the optimal "precision therapeutic" for these patients will be a highly selective JAK1 inhibitor.

In conclusion, we have described the first humans carrying a germline GoF mutation in *JAK1*. Using a precision medicine approach,¹⁰ oral therapy with ruxolitinib resulted in remarkable improvement in key clinical end points. This characterization of a human *JAK1* GoF mutation expands our understanding of the role of JAK1 in eosinophil biology, hematopoiesis, and immune function, and provides further justification for the consideration

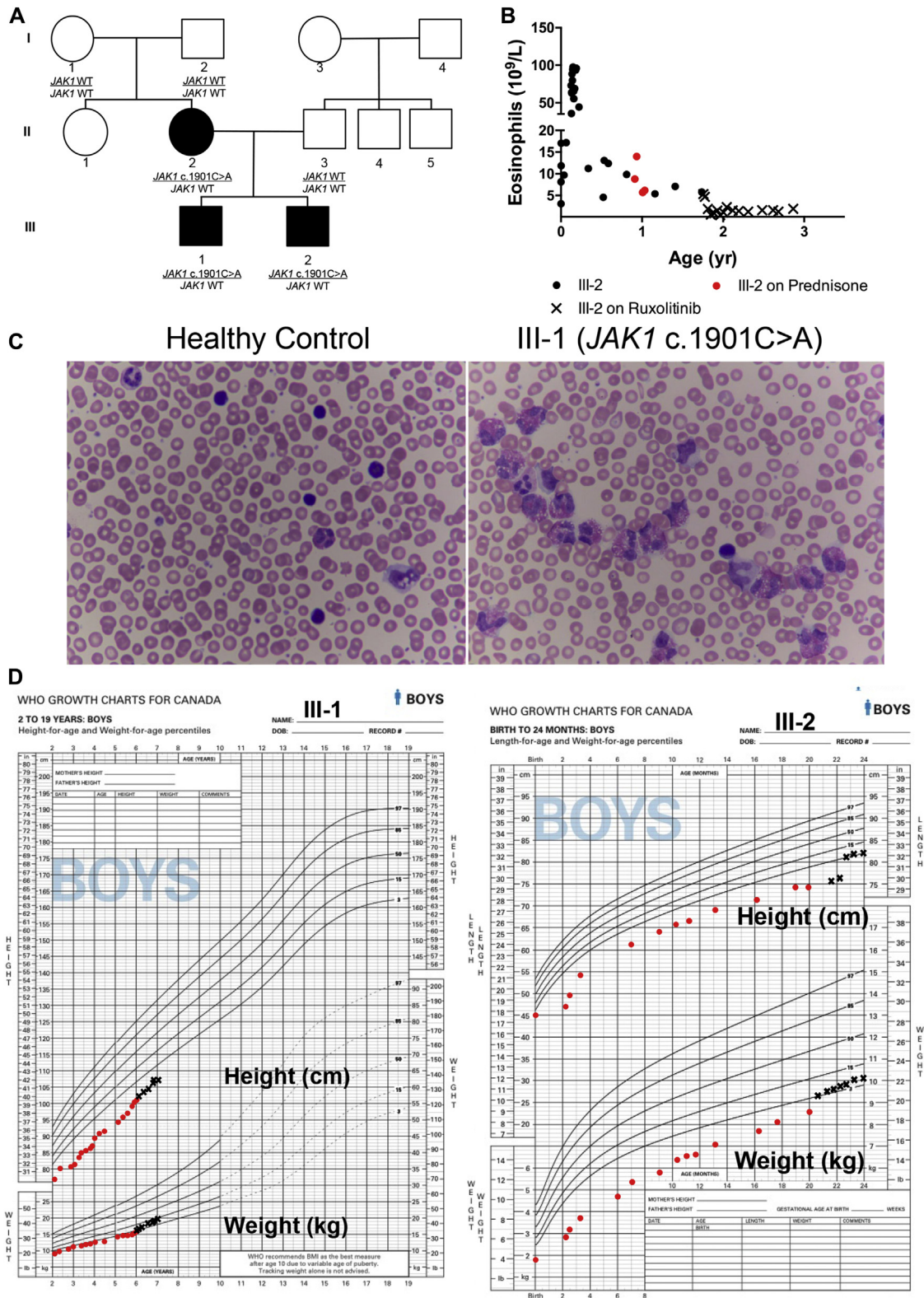


FIG 1. Family pedigree and clinical phenotypic features of the *JAK1* c.1901C>A mutation. **A**, Family pedigree. **B**, Absolute eosinophil counts for patient III-2 since birth until present. Normal range is less than $0.5 \times 10^9/L$ and hyper-eosinophilia is defined as blood eosinophilia ($\geq 1.5 \times 10^9/L$) for longer than 6 months. Red ● indicates eosinophil counts while receiving systemic corticosteroids, and black X indicates eosinophil counts while on ruxolitinib. **C**, Blood smear of patient III-1 showing profound eosinophilia compared with the healthy control. **D**, Growth charts for patients III-1 and III-2 demonstrate profound failure of both linear growth and weight gain, which improves rapidly after starting ruxolitinib. Growth after starting ruxolitinib is denoted by an x.

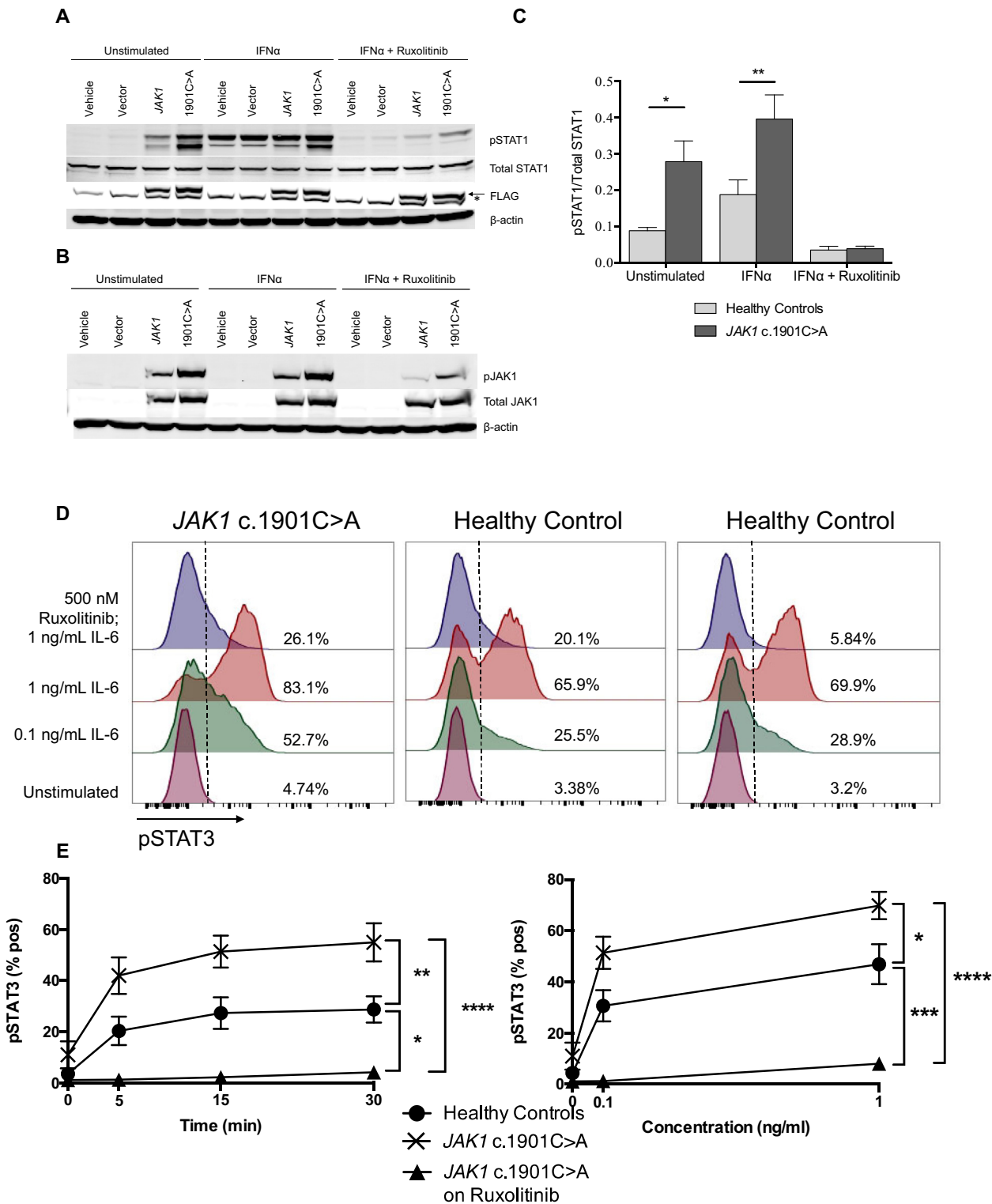


FIG 2. Characterization of the JAK1 p.A634D mutation. **A** and **B**, HEK293 cells transfected with a plasmid carrying the JAK1 c.1901C>A mutation show increased pJAK1 and pSTAT1 after 100U IFN- α stimulation for 30 minutes. Cells pretreated with ruxolitinib (500 nM; 1 hour) before stimulation showed decreased JAK1 and STAT1 activity. FLAG and β -actin were used as loading controls. *Nonspecific bands. **C**, Quantification of pSTAT1 relative to total STAT1 in 2 healthy controls and 3 patient-derived EBV-immortalized B-cell lines across 4 technical replicates with or without IFN- α stimulation (10U for 30 minutes). Pretreatment with ruxolitinib (500 nM; 1 hour) decreased STAT1 phosphorylation in response to IFN- α stimulation. Statistical analysis was performed using 2-way ANOVA with a Bonferonni posttest. **D**, STAT3 phosphorylation was measured in CD3⁺ T cells from whole blood in patients and healthy controls after IL-6 (0.1 and 1 ng/mL) treatment for 30 minutes. Pretreatment with ruxolitinib (500 nM) decreased pSTAT3 activation. **E**, pSTAT3 response in CD3⁺ T cells from patient and healthy controls over a time course (0.1 ng/mL of IL-6) and a dose response (15 minutes). Statistical analysis performed by 2-way ANOVA, using Tukey to correct for multiple comparisons using 7 healthy controls, 3 patient samples across 5 separate blood draws and 3 treated samples. * $P < .05$, ** $P < .01$, *** $P < .001$, **** $P < .0001$.

of JAK inhibitors to treat more common multifactorial conditions such as atopic dermatitis and eosinophilic disorders.

Kate L. Del Bel, MSc^{a,*}
Robert J. Ragotte, BSc^{a,*}
Aabida Saferali, MSc^a
Susan Lee, RN^a
Suzanne M. Vercauteren, MD, PhD^b
Sara A. Mostafavi, PhD^c
Richard A. Schreiber, MD^a
Julie S. Prendiville, MD^a
Min S. Phang, MD^a
Jessica Halparin, MD^a
Nicholas Au, MD^b
John M. Dean, MD, BS^a
John J. Priatel, PhD^b
Emily Jewels, RN^a
Anne K. Junker, MD^a
Paul C. Rogers, MB ChB, MBA^a
Michael Seear, MB ChB^a
Margaret L. McKinnon, MD^c
Stuart E. Turvey, MBBS, DPhil^a

From the Departments of ^aPediatrics, ^bPathology and Laboratory Medicine, and ^cMedical Genetics, British Columbia Children's Hospital, University of British Columbia, Vancouver, British Columbia, Canada. E-mail: mmckinnon@cw.bc.ca. Or: sturvey@cw.bc.ca.

*These authors contributed equally to this study.

S. E. Turvey holds the Aubrey J. Tingle Professorship in Pediatric Immunology and is a clinical scholar of the Michael Smith Foundation for Health Research. This work was supported in part by funding from the Canadian Institutes of Health Research and the Canadian Allergy, Asthma and Immunology Foundation.

Disclosure of potential conflict of interest: S. E. Turvey receives grant support from Michael Smith Foundation for Health Research, Canadian Institutes of Health Research, and Canadian Allergy, Asthma and Immunology Foundation. The rest of the authors declare that they have no relevant conflicts of interest.

REFERENCES

- O'Shea JJ, Schwartz DM, Villarino AV, Gadina M, McInnes IB, Laurence A. The JAK-STAT pathway: impact on human disease and therapeutic intervention. *Annu Rev Med* 2015;66:311-28.
- Loh ML, Tasian SK, Rabin KR, Brown P, Magoon D, Reid JM, et al. A phase 1 dosing study of ruxolitinib in children with relapsed or refractory solid tumors, leukemias, or myeloproliferative neoplasms: a children's oncology group phase 1 consortium study (ADVL1011). *Pediatr Blood Cancer* 2015;62:1717-24.
- Flex E, Petrangeli V, Stella L, Chiaretti S, Hornakova T, Knoops L, et al. Somatic acquired JAK1 mutations in adult acute lymphoblastic leukemia. *J Exp Med* 2008;205:751-8.
- Hornakova T, Chiaretti S, Lemaire MM, Foa R, Ben Abdelali R, Asnafi V, et al. ALL-associated JAK1 mutations confer hypersensitivity to the antiproliferative effect of type I interferon. *Blood* 2010;115:3287-95.
- Springuel L, Hornakova T, Losdyck E, Lambert F, Leroy E, Constantinescu SN, et al. Cooperating JAK1 and JAK3 mutants increase resistance to JAK inhibitors. *Blood* 2014;124:3924-31.
- Kleppe M, Soulier J, Asnafi V, Mentens N, Hornakova T, Knoops L, et al. PTPN2 negatively regulates oncogenic JAK1 in T-cell acute lymphoblastic leukemia. *Blood* 2011;117:7090-8.
- Hornakova T, Staerk J, Royer Y, Flex E, Tartaglia M, Constantinescu SN, et al. Acute lymphoblastic leukemia-associated JAK1 mutants activate the Janus kinase/STAT pathway via interleukin-9 receptor alpha homodimers. *J Biol Chem* 2009;284:6773-81.
- Yasuda T, Fukada T, Nishida K, Nakayama M, Matsuda M, Miura I, et al. Hyperactivation of JAK1 tyrosine kinase induces stepwise, progressive pruritic dermatitis. *J Clin Invest* 2016;126:2064-76.
- Sabrautski S, Janas E, Lorenz-Depiereux B, Calzada-Wack J, Aguilar-Pimentel JA, Rathkolb B, et al. An ENU mutagenesis-derived mouse model with a dominant Jak1 mutation resembling phenotypes of systemic autoimmune disease. *Am J Pathol* 2013;183:352-68.
- Jameson JL, Longo DL. Precision medicine—personalized, problematic, and promising. *N Engl J Med* 2015;372:2229-34.

Available online January 19, 2017.

<http://dx.doi.org/10.1016/j.jaci.2016.12.957>

Niacin intake and incident adult-onset atopic dermatitis in women



To the Editor:

Adult-onset atopic dermatitis (AD) is a recognized entity,¹ but little is known about risk factors for its development. Results from a randomized controlled trial of coated oral nicotinamide tablets for the prevention of skin cancer found that nicotinamide modestly decreased transepidermal water loss (TEWL), a measure of epidermal barrier integrity, among participants.² Nicotinamide is a derivative of niacin (vitamin B₃, nicotinic acid), a nutrient found in many foods and supplements, including B vitamin complex and multivitamins. Given that increases in TEWL are associated with AD,³ we hypothesized that increased niacin intake would be protective from the development of AD in adulthood. We aimed to investigate this association in the Nurses' Health Study 2 (NHS2), a large prospective cohort study of US female nurses.

NHS2 was established in 1989 with 116,430 participants between the ages of 25 and 42 years. Follow-up questionnaires are sent biennially to participants, updating information on diseases, anthropometric factors, and other risk factors. Height and race/ethnicity were assessed at cohort baseline. Smoking status, physical activity, postmenopausal hormone use, and history of asthma, hypertension, hypercholesterolemia, type 2 diabetes, and cardiovascular disease (myocardial infarction and stroke) are all assessed and updated during cohort follow-up.

AD was assessed by self-report in 2013 when participants were asked about a history of clinician-diagnosed "eczema (atopic dermatitis)," in addition to the year they were diagnosed in intervals (before 1995, 1995-2002, 2003-2008, 2009-2010, 2011+). In this analysis, we included only incidence cases with reported diagnosis after 1995. Cases of AD diagnosed before 1995, when participants were between the ages of 31 and 48 years, were excluded.

A validated food frequency questionnaire was used to collect dietary information in 1991 and every 4 years thereafter.^{4,5} Participants responded to questions regarding how often on average they consumed specific types of food and drink, including alcohol, during the previous year. Total niacin intake was calculated using intake from both dietary sources and supplements using cumulative average intake up to the start of each follow-up interval to represent long-term dietary intake and to reduce measurement errors.

We followed participants for incident AD starting from 1995. Participants who reported AD diagnosed before 1995, who did not return the 2013 questionnaire, and those missing niacin intake information were excluded, leaving 67,643 participants in the analysis. Person-time of follow-up was calculated from the return month of the 1995 questionnaire to the date of the first report of AD or end of follow-up (June 2013), whichever came first.

Cox proportional hazard models were used to compute the hazard ratios and 95% CI of AD with total, dietary, and supplemental niacin intakes in quintiles. A separate analysis was conducted with B vitamin complex and multivitamin intake as the exposures. Covariates used in multivariate analyses are listed in the table legends. The most recent information for time-varying variables before each follow-up interval was used to take into account potential changes over the follow-up. Trend tests were performed by assigning median values for niacin intake categories and treating the new variable as a continuous term in

METHODS

Ethical considerations

Research study protocols were approved by our institutional review board. Four members of the family (the affected children and their parents) were enrolled. Written informed consent for genetic testing and participation was provided by the parents for their children.

Exome sequencing

Clinical diagnostic exome sequencing of the affected children and their parents was performed commercially from whole blood samples (Ambyr Genetics, Aliso Viejo, Calif) using a published approach.^{E1} Whole blood sample collection was conducted as per Ambyr protocol: 6 to 10 cc for adults, and 5 cc for children in an EDTA tube. The Ambyr Genetics Clinical Diagnostic Exome uses the Agilent SureSelect Target Enrichment System or the Roche NimbleGen SeqCap EZ VCRome 2.0 capture systems for sample preparation and paired-end sequencing on the Illumina HiSeq 2000 or HiSeq 2500. Data are annotated using the Ambyr Variant Analyzer tool (AVA). Analytical range of the data is high, with approximately 90% of the bases expected to have quality scores of Q20 or higher, equivalent to a base-calling error rate of 1:100; thus, approximately 90% of the exome is predicted to be covered at 10X or higher. Sequence undergoes bioinformatic analysis, filtering according to appropriate inheritance models (autosomal-dominant, X-linked recessive, X-linked dominant models, autosomal-recessive), followed by manual review to rule out sequencing artifacts and polymorphisms along with medical interpretation to rule out genes lacking clinical overlap in the patient's evaluated phenotype. Candidate variants were validated at Ambyr genetics via Sanger methods and segregation analysis was performed in the family. A second possibly pathogenic heterozygous variant was detected in *FGR* (FGR proto-oncogene, Src family tyrosine kinase), but using familial cosegregation analysis in the maternal grandparents, only the *JAK1* variant proved to appropriately segregate with the clinical phenotype.

Quantification of *JAK1* gene and protein expression

A protein model was constructed using Swiss-Prot to portray the location of the altered amino acid within the JAK1 protein.^{E2,E3} Total RNA was isolated from whole blood using a RiboPure Blood kit (Thermo Fisher Scientific, Ontario, Canada), transcribed to cDNA (iScript, Bio-Rad, Ontario, Canada) and *JAK1* gene expression was measured by SYBR Green qPCR (Universal SYBR Green Super Mix, Bio-Rad) using gene-specific primers for *JAK1* (Table E2, PrimeTime primers, IDT, San José, Calif) and housekeeping gene *ACTB*. Reactions were run using a ViaA7 Real-Time PCR System (Applied Biosystems, Carlsbad, Calif) and relative gene expression was analyzed by using the $2^{-\Delta\Delta Ct}$ Livak method.^{E4}

Immunoblotting was carried out to study JAK1 protein expression using standard protocols.^{E5} In brief, immortalized B-cell lysates were generated with modified RIPA buffer (50 mM Tris-HCl, 150 mM NaCl, 2 mM EGTA and EDTA, and 1% TritonX-100 at pH 7.5) supplemented with Halt protease and phosphatase inhibitor cocktail (Thermo Fisher Scientific). The total protein concentration of the lysates was measured by a modified Bradford assay (Coomassie Plus Assay kit, Thermo Fisher Scientific) and adjusted accordingly. SDS-PAGE (10%) was performed to separate proteins, which were then transferred onto a polyvinylidene difluoride membrane (Immobilon-FL, EMD Millipore, Billerica, Mass). The membranes were blocked and blotted with various primary antibodies: anti-JAK1 (Abcam, Cambridge, Mass), anti- β -actin (Cell Signaling Technology, Danvers, Mass). They were subsequently blotted with fluorescently labeled secondary antibodies and imaged by a LI-COR Odyssey infrared image system (LI-COR Bioscience, Lincoln, Neb). The JAK1 expression was quantified by

analyzing the band densitometry (ImageJ freeware) normalized for β -actin expression.

Cloning and transfection studies

Plasmids used for transfection studies contained full-length *JAK1* cloned into pCMV6-Entry with a C-terminal Myc-DDK (FLAG) tag (Origene, Rockville, Md). The *JAK1* gene was reverse transcribed from mRNA extracted from patient EBV-immortalized B cells and a *JAK1* gene-specific primer (SuperScript III reverse transcriptase kit, Thermo Fisher Scientific) (Table E2). The *JAK1* gene was amplified using the Phusion High Fidelity PCR kit (New England Biolabs, Ipswich, Mass) and inserted into the pCMV6-Entry vector using AsiSI and MluI restriction digest sites (New England Biolabs). A *JAK1* c.1901C>A construct was made using the Q5 site-directed mutagenesis kit (New England Biolabs) and primers designed using the NEBaseChanger. Sequencing was used to confirm both the cloning of the gene and the mutation. Plasmids were purified (QIAprep Spin miniprep kit, Qiagen, Ontario, Canada) and used to transfect HEK293 cells. Cells were seeded at 2.5×10^5 cells/well in a 12-well plate with 1 mL of Dulbecco modified Eagle medium with 10% FCS and incubated for 24 hours at 37°C. Cells were transfected with 2 μ g of plasmid DNA using Lipofectamine 2000 (Thermo Fisher Scientific, Waltham, Mass). Cells were incubated overnight for 24 hours. Cells were stimulated with 100U of IFN- α (PBL Assay Science, Piscataway, NJ) for 30 minutes with or without 60 minutes of pretreatment with 500 nM of ruxolitinib (Cedarlane, Burlington, Canada). Cells were washed before being lysed and blotted as described above. In addition to anti- β -actin, anti-JAK1 and anti-pJAK1 (Tyr1022 and Tyr1023) (Abcam, Cambridge, Mass), antibodies to FLAG (Santa Cruz Biotechnology, Dallas, Tex) and anti-STAT and anti-pSTAT1 (Tyr701) (Cell Signaling Technology, Danvers, Mass) were used.

Characterization of the GoF phenotype

To characterize the GoF phenotype, EBV-immortalized B cells from the patients were stimulated as above with IFN- α (10U) with or without pretreatment of ruxolitinib (500 nM). Cell lysates were immunoblotted as above using antibodies for STAT1, pSTAT1 (Tyr701), and β -actin (Cell Signaling Technology, Danvers, Mass).

The mutation was further characterized in primary cells using whole blood samples. Blood was collected in heparinized tubes and stimulated with IL-6 (0.1-1.0 ng/mL) for 5, 15, or 30 minutes with or without 60 minutes of ruxolitinib (500 nM) pretreatment. Cells were surface stained with anti-CD3, anti-CD8, anti-CD14, anti-CD16, anti-CD49d, and anti-CD19 (BD Biosciences). Cells were fixed and permeabilized per manufacturer's instructions (Lyse/Fix buffer and Perm II, BD Biosciences, Ontario, Canada) and stained with pSTAT3 (BD Biosciences). pSTAT3 activity was compared between stimulated and nonstimulated cells in patient and healthy control cells. All flow cytometry experiments were performed on an LSRII instrument (BD Biosciences) and analyzed using FlowJo software (TreeStar, Ashland, Ore).

REFERENCES

- Farwell KD, Shahmirzadi L, El-Khechen D, Powis Z, Chao EC. Enhanced utility of family-centered diagnostic exome sequencing with inheritance model-based analysis: results from 500 unselected families with undiagnosed genetic conditions. *Gent Med* 2015;17:578-86.
- Guex N, Peitsch MC. SWISS-MODEL and the Swiss-PdbViewer: an environment for comparative protein modeling. *Electrophoresis* 1997;18:2714-23.
- Toms AV, Deshpande A, McNally R, Jeong Y, Rogers JM, Kim CU. Structure of a pseudokinase-domain switch that controls oncogenic activation of Jak kinases. *Nat Struct Mol Biol* 2013;20:1221-3.
- Livak KJ, Schmittgen TD. Analysis of relative gene expression data using real-time quantitative PCR and the $2^{-\Delta\Delta Ct}$ method. *Methods* 2001;25:402-8.
- Kumar P, Henikoff S, Ng PC. Predicting the effects of coding non-synonymous variants on protein function using the SIFT algorithm. *Nat Protocols* 2009;4:1073-81.

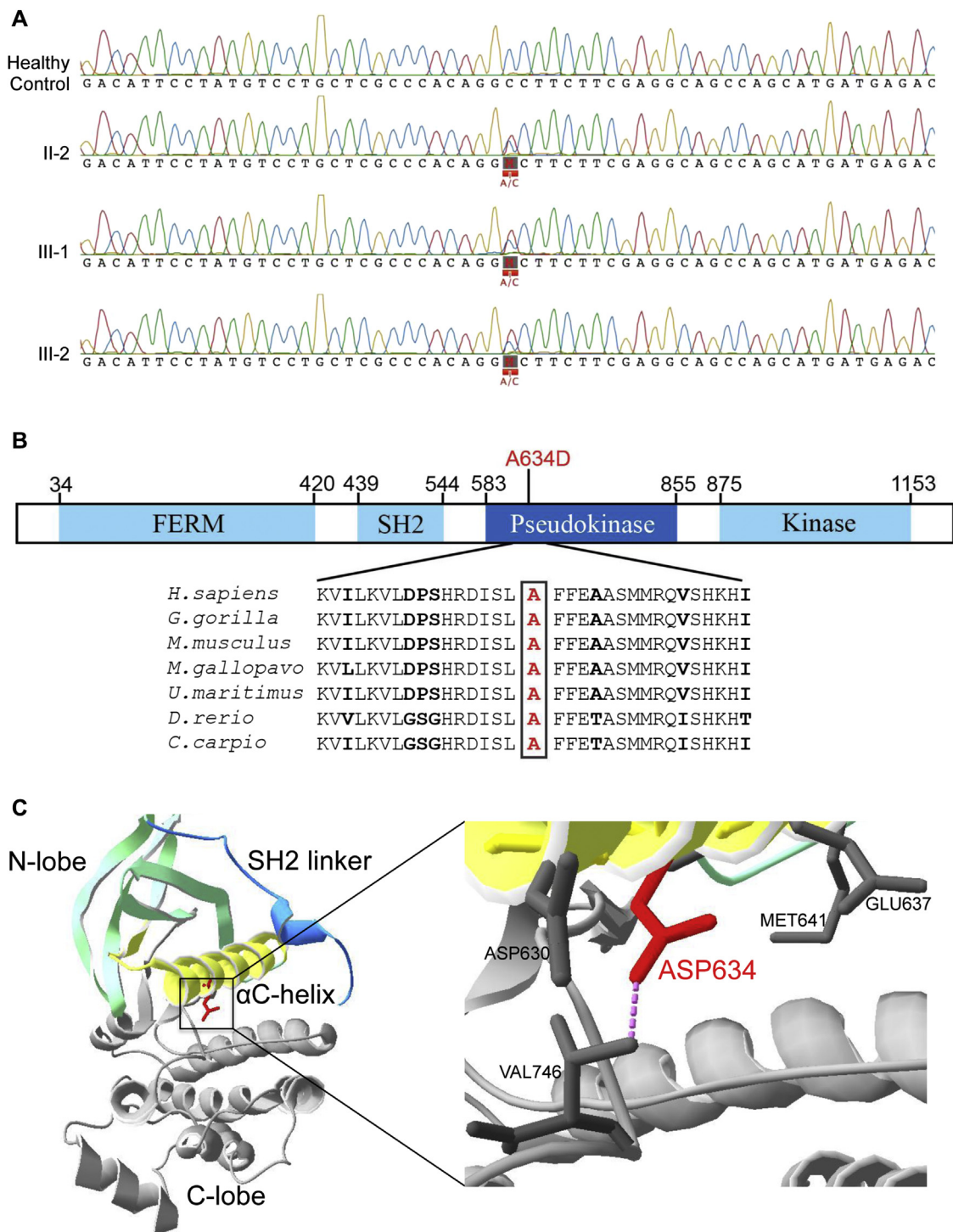


FIG E1. The *JAK1* c.1901C>A (p.A634D) mutation. **A**, Sanger sequencing of whole blood from the patients and a healthy control showing that the patients are heterozygous for the *JAK1* c.1901C>A mutation. **B**, Structure of *JAK1* protein showing the location of the p.A634D mutation within the pseudokinase domain. Multiple sequence alignment of the *JAK1* p.A634D region showing conservation across species. **C**, Crystal structure of the *JAK1* pseudokinase domain showing the position of the A634D mutation within the α C helix.

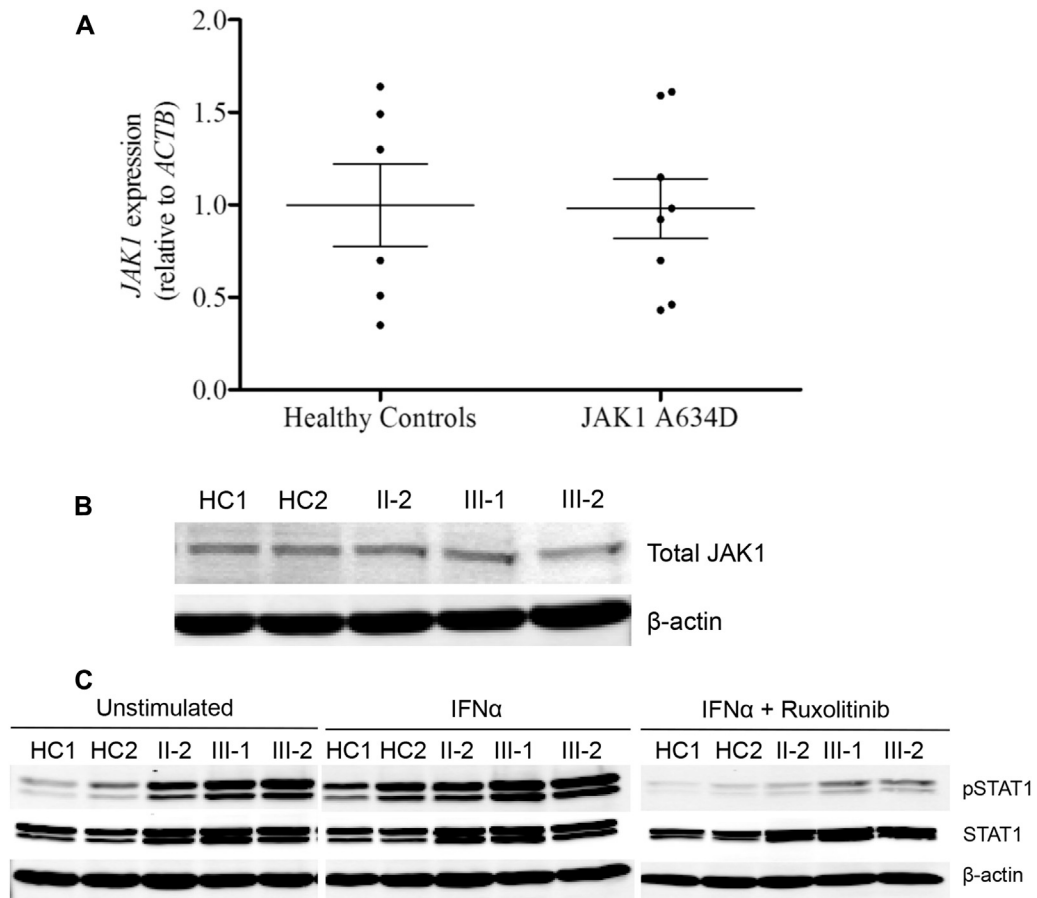


FIG E2. Characterization of the JAK1 p.A634D mutation. *JAK1* c.1901C>A mutation does not affect its own expression at the mRNA (**A**) or protein level (**B**). **C**, Immunoblotting on EBV-immortalized B cells at baseline, after stimulating with IFN- α (10 U/mL for 30 minutes), and after inhibition with ruxolitinib (500 nM; 1 hour), comparing healthy control cells (HC) to JAK1 A634D patient cells.

TABLE E1. Clinical features associated with autosomal-dominant *JAK1* GoF mutations

Hematologic abnormalities	Eosinophilia
Autoimmunity	Autoimmune hypothyroidism
Atopy	Asthma
	Atopic dermatitis
	Food allergy
	Environmental allergies
Infections	Recurrent viral infections
Organ involvement	Hepatosplenomegaly
	Prenatal liver cysts
	Eosinophilic infiltration of the gastrointestinal tract
Growth abnormalities	Failure to thrive (pediatric)
	Short stature (adult)
Treatments and response	Corticosteroids (poor response)
	Ruxolitinib (favorable response)

TABLE E2. Primer sequence

Primer name	Primer (5'-3')	Primer direction
<i>JAK1</i> cloning	CGC CGC GAT CGC CAT GCA GTA TAT AAA	Forward
	CGC GTA CGC GTT TTT AAA AGT GCT TCA	Reverse
<i>JAK1</i> genomic sequencing	GGA TCT GGT GCA GGG CGA GC	Forward
	GTC GCG GAC ACA GAC GCC AT	Reverse
<i>ACTB</i> housekeeping gene	GTT GCG TTA CAC CCT TTC TT	Forward
	ACC TTC ACC GTT CCA GTT T	Reverse
<i>JAK1</i> qPCR (exon 5-6)	ATC CCT AGA CAC TCG TTC TCA	Forward
	TCA CTG GAG TAT CTG TTT GCT C	Reverse